

“Incidentalomas” on MR imaging examinations of the adult knee.

A pictorial essay

Konstantinos Pikoulas, Georgios Giannikouris, Ioanna Staikidou, Georgios Mantzikopoulos
Radiology Department, KAT Hospital, Kifissia, Greece

SUBMISSION: 1/7/2020 - ACCEPTANCE: 13/10/2020

ABSTRACT

Musculoskeletal radiologist’s practice includes a great deal of magnetic resonance imaging (MRI) examinations of the knee. The patient is referred for MRI mainly because of knee pain. The examination may reveal the cause of pain, but there may be additional findings discovered, that are not associated with the patient’s symptoms at all. These incidental findings may be referred to as “incidentalomas”. Although, by definition, incidentalomas are not the cause of patient’s symptoms and signs at the time of their discovery, some of these le-

sions may be misinterpreted, may have other clinical implications or may eventually become symptomatic. The purpose of this pictorial essay is twofold. First to present incidentalomas that are clinically unremarkable and the diagnosis is clear. Second to alert the radiologist on the incidentalomas that may have clinically significant consequences, such as tumours with malignant potential or increased risk of fractures, abnormal muscles in close proximity with vital structures, or findings indicative of systemic disease.



KEY WORDS

Magnetic Resonance Imaging; Knee joint; Bone neoplasms; Tendons; Connective tissue; Incidental findings



CORRESPONDING AUTHOR, GUARANTOR

Konstantinos Pikoulas, Radiology Department, KAT Hospital, 2 Nikis Str, 14561 Kifissia, Greece, Email: k_pikoulas@yahoo.gr

Introduction

Pain is the most common symptom for which the clinicians refer a patient for a knee MRI examination, and internal derangement of the joint is the usual condition to be evaluated. In a high percentage of patients, imaging findings correlate well with patients' symptoms and clinical findings. Apart from the clinically relevant, unexpected imaging findings may be revealed that are not related to the patient's symptoms. These findings are incidental and most of the times they are considered “do not touch lesions”, as they do not have clinical significance. In some cases, though, the revealed unexpected findings may have significant consequences on patient's health, such as potentially malignant tumours, aberrant muscles abutting on adjacent structures, findings of previous traumatic or inflammatory conditions, or manifestations of systemic diseases. In this pictorial essay, we present our experience on cases of “incidentalomas” on knee MRI examinations. With this essay, we aim to familiarise radiologists with knee incidentalomas and to alert them on the entities that may have clinically significant consequences.

Discussion

Incidentalomas may be revealed on every anatomic structure shown on a knee MRI examination. An efficient way not to miss them is to inspect the anatomic structures one by one following a structured approach, i.e. osseous lesions, intraarticular lesions, and extraarticular lesions.

Osseous lesions

The bones should be the first to be inspected. **Osseous tumours** are included among the unexpected lesions when they are clinically silent. Generally, incidentally found bone tumours are benign, but in some cases there may be serious consequences such as fractures or malignant transformation. If a bone tumour is revealed on MRI for the first time, it is mandatory to correlate the MRI findings with plain radiographs and/or computed tomography (CT).

Enostosis (also called bone island) is frequently identified on knee MRI examinations. It represents a focus of compact bone located in cancellous bone. The metaphysis of long bones is the preferred location [1]. An enostosis is usually oval in shape, and on MRI it demonstrates uniformly low signal intensity on all sequences, due to

lack of free protons. The signal of the adjacent bone marrow is normal. A sclerotic metastasis, which is the main differential diagnosis, has smooth periphery while an enostosis may show trabeculated margins. Additionally, bone marrow adjacent to a metastasis may present aggressive findings such as marrow oedema, periostitis and cortical breaching. Enostoses do not enhance after intravenous contrast administration [2]. A subchondral location should not raise suspicion of an osteochondral lesion, because of the absolute similarity of signal intensity to compact bone (**Fig. 1**). Multiplicity of lesions is called “osteopoikilosis” [1].

Cartilage forming tumours, found unexpectedly on knee MRI examinations, are usually benign. **Enchondromas** are located centrally in the metaphysis of long bones. They have distinct lobulated margins and shallow endosteal scalloping. Eccentric subcortical lesions do not breach the cortex [3]. On MRI they are incidentally found in about 3.5% of patients [4]. Signal intensity is high on T2W images and low on T1W images. The matrix of the lesion contains foci of low signal intensity, representing the rings-arcs-floccules calcifications shown on plain radiographs and CT (**Fig. 2**). Multiplicity of the lesions is a rare condition called Ollier's disease. If an enchondroma enlarges to replace enough trabeculae, the bone weakens and a fracture may occur [3].

Osteochondroma is eccentrically located. It is a lesion of the osseous surface and grows away from the bone, towards the adjacent soft tissue. It represents a bone extrusion, thus the term “exostosis” is also used [5]. Characteristically the cortex of the exostosis shows absolute continuity with the osseous cortex and the matrix blends with the bone marrow. A cartilaginous shell covers the cap of the lesion. On MRI, the shell shows high signal intensity on cartilage specific sequences, i.e. PDW or gradient echo with fat suppression images. When the cartilaginous shell calcifies, signal intensity drops [6]. During adolescence, osteochondromas enlarge and may cause symptoms due to pressure of adjacent anatomical structures (**Fig. 3**). Following a contact injury, they may fracture. Multiple skeletal lesions are a manifestation of the “hereditary multiple exostoses”, an autosomal dominant hereditary disorder. Enchondromas and osteochondromas may undergo malignant transformation [3, 5].

A **fibrous cortical defect** is the commonest benign bone tumour. It is estimated that it is present in about

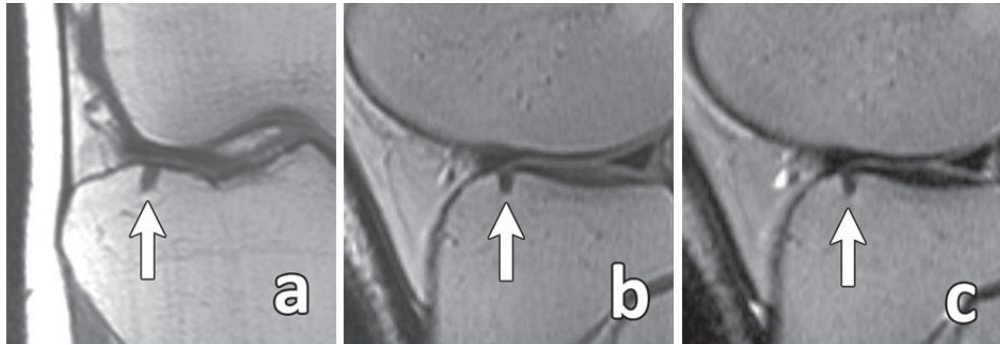


Fig. 1. a: coronal T1W/SE, **b:** sagittal PDW/SE, **c:** sagittal T2W/SE. A female 46-year-old patient, followed up for chondromalacia. There is a subarticular lesion at the lateral tibial plateau (arrows). It manifests low signal intensity on all pulse sequences. Findings are consistent with enostosis.

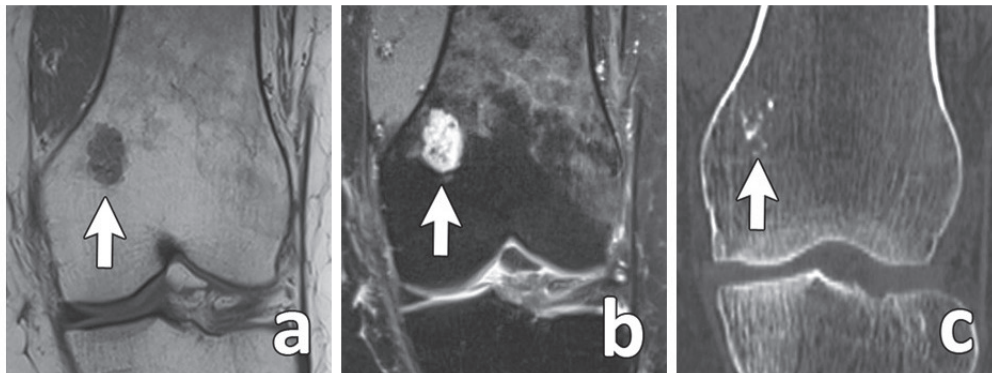


Fig. 2. a: coronal T1W, **b:** coronal PDW with fat saturation, **c:** coronal CT reformation. A female 42-year-old patient, smoker, referred for knee blocking. A medially located lobulated lesion shows low signal intensity on T1W (arrow in **a**) and high signal intensity on PDW (arrow in **b**) image. It shows intralesional low signal foci which correspond to the calcifications on the coronal CT reformation (arrow in **c**). Findings are consistent with enchondroma. There is diffuse signal alteration of the bone marrow at the distal femoral metadiaphysis consistent with marrow reconversion.

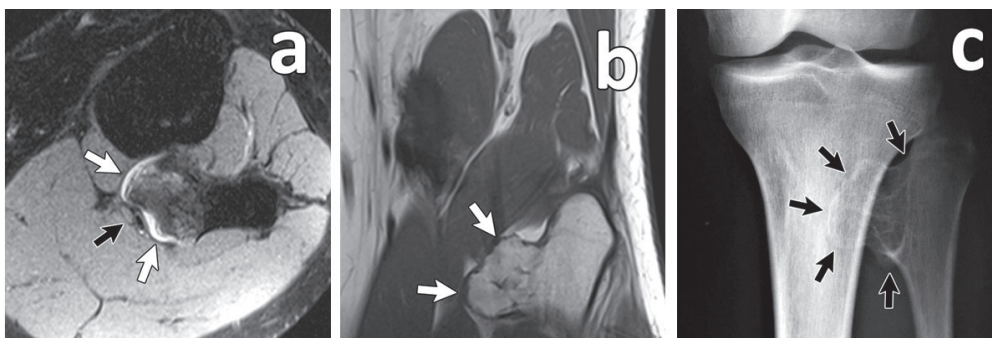


Fig. 3. a: axial PDW with fat saturation, **b:** coronal T1W (fibula level), **c:** anteroposterior radiograph. A 16-year-old female patient with anterior knee pain. An osteochondroma of the fibula is incidentally found, projecting medially. The margins are lobulated (white arrows in **a** and **b**). The matrix shows inhomogeneous high signal intensity on the axial image. The cartilaginous shell shows high signal intensity and has a few millimeters thickness (white arrows in **a**). Due to close proximity of the lesion with the popliteal vessels (black arrow in **a**) there is increased risk of impingement and probable peripheral ischaemia. On the corresponding radiograph, the continuation of the lesion's margins with the bone cortex is clearly depicted (black arrows in **c**). Note the rings and arcs calcifications as well.

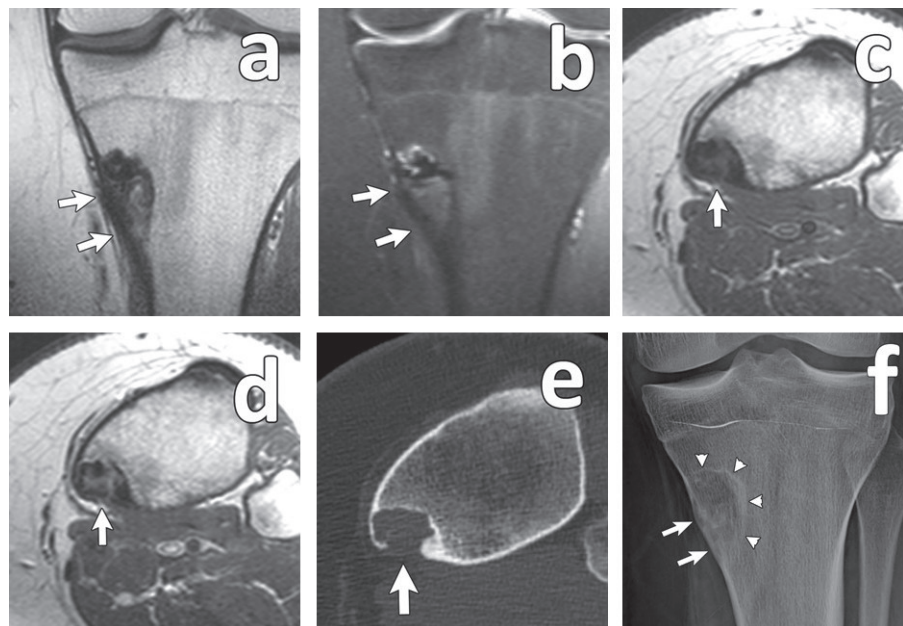


Fig. 4. **a:** coronal T1W, **b:** coronal PDW with fat saturation, **c:** axial T1W, **d:** axial T1W with contrast, **e:** axial CT, **f:** anteroposterior radiograph. A 16-year-old male patient with anterior knee pain. An eccentric lesion originates from the bone cortex, and the tibia is slightly expanded (arrows in **a**, **b**, and **f**). It shows mixed signal intensity on T1W and T2W. The cortex is breached (arrows in **c**, **d**, **e**), but no soft tissue mass is identified. The adjacent bone marrow is normal. The lesion shows moderate enhancement. On the radiograph, the lesion appears osteolytic, partially calcified, and it is surrounded by a sclerotic border (arrowheads). The findings are consistent with non-ossifying fibroma because its longitudinal dimension exceeds 3 cm.

30% of children. Fibrous cortical defects are generally not seen in adults over 30 years. They may be associated, especially if multiple, with neurofibromatosis type 1 and Jaffe-Campanacci syndrome [6]. A fibrous cortical defect has an intracortical location. Histologically it shows benign fibroblastic proliferation admixed with osteoclast-type giant cells [7]. The size of a fibrous cortical defect extends up to 3 cm. Over this dimension, it is defined as a **non-ossifying fibroma**. Both lesions show low signal on MRI due to the presence of fibrous matrix. In some cases, they may reveal high signal intensity on T2W images due to the presence of scarce hypercellular fibrous tissue and massive aggregation of foamy histiocytes [8]. The lesion is surrounded by a hypointense rim, which represents the marginal sclerosis seen on plain radiographs or CT (**Fig. 4**). After intravenous gadolinium injection, the matrix of the lesion shows various grades of enhancement [8]. The overlying cortex may be thinned or even breached but there is no soft tissue mass identified [9]. During osseous growth, the lesions eventually start to ossify from their diaphyseal

side. The ossification progressively continues in a centripetal fashion, until the whole lesion becomes homogeneously sclerotic [10].

A **cortical desmoid** represents an avulsive lesion at the insertion of the medial head of gastrocnemius muscle, producing a defect with subsequent fibrous repair [11]. It is usually found in young active adolescents, and is one of the most frequent incidental findings on knee MRI examinations. At the early stages MRI findings of cortical irregularity and bone and soft tissue oedema may be considered as manifestations of a neoplastic process. Radiography and CT will confirm the benign nature of this entity [12].

Intraosseous lipomas are considered rare tumours [13]. They are benign and their matrix is composed of mature fat cells interspersed with small quantities of fibrous and vascular tissue. Fat necrosis and dystrophic calcification may be seen. Usually an intraosseous lipoma is surrounded by a sclerotic margin. On MRI, the signal intensity of the lesion equals the signal intensity of bone marrow (**Fig. 5**). A low signal intensity rim

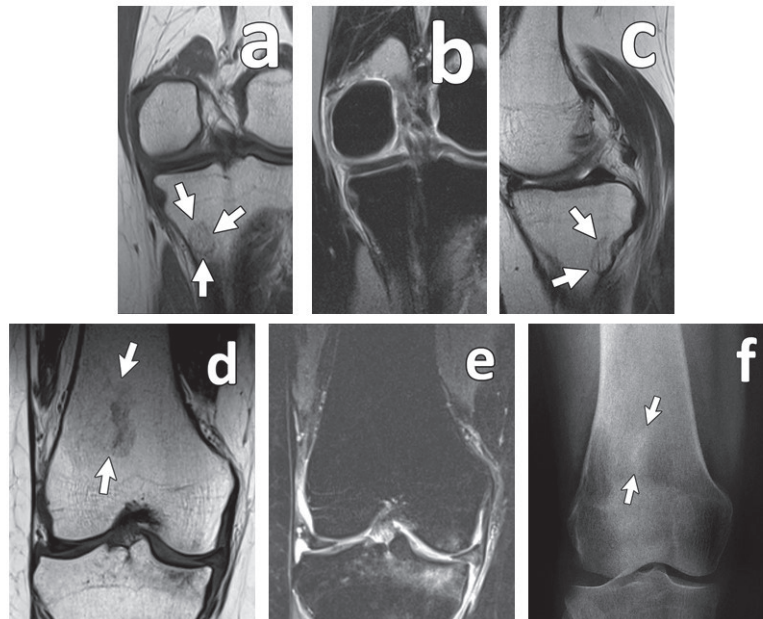


Fig. 5. a: coronal T1W, **b** coronal PDW with fat saturation, **c:** sagittal T2W. A 53-year-old female patient referred for probable meniscus tear. A lesion is disclosed, eccentrically situated at the posterior region of the tibial metaphysis. It has signal intensity that equals the signal of bone marrow on all sequences. Low signal lines are traversing the lesion vertically, representing bony trabeculae. A low signal margin is surrounding the lesion (white arrows). Findings are consistent with an intraosseous lipoma. **d:** coronal T1W, **e:** coronal PDW with fat saturation, and **f:** anteroposterior radiograph. A 67-year-old female patient with recent knee injury. Apart from the obvious signs of injury an unexpected lesion is revealed, located at the lateral part of the femoral metaphysis. The signal intensity of the lesion equals the signal of bone marrow. The femur is slightly expanded. A faint low signal margin is surrounding the lesion (arrows in **d**). On the T1W image, a portion of lesion's matrix has low signal and corresponds to the faint calcification shown on the radiograph (arrows in **f**). Findings are consistent with an intraosseous lipoma.

surrounds the lesion, separating it from the adjacent bone marrow [14]. Bone trabeculae are replaced in various degrees, the commonest appearance being the total lack of trabeculae. A lipoma may be difficult to appreciate if a significant percentage of trabeculae is present due to lack of striking signal difference between the lesion and the rest of the bone. A low signal intensity rim is depicted in 74% of cases [14]. The host bone may be expanded but the cortex remains intact [15] (**Fig. 5**).

The bones of the adult skeleton are composed of **fat-tty marrow**. By the 25th year of age no haematopoietic marrow should exist at the level of the knee joint. Diffuse signal alteration of the metaphyseal bone marrow, suggestive of marrow reconversion, can be related to an occult disorder, such as obesity, diabetes, chronic conditions related to anaemia, treatment with haematopoietic growth factors. If no underlying disease is discovered, other causes should be considered, such as heavy smoking or large oxygen debt sports (long-dis-

tance running or free diving) [16] (**Fig. 2**).

The **patella** is the largest sesamoid bone in the skeleton and has a discoid shape. Multiple ossification nuclei coalesce rapidly and the patella ossifies between 3 and 5 years [17]. Additional ossification centers may develop. Failure of unification of a secondary ossification center results in a **bipartite patella**. The commonest part of segmentation failure involves the superolateral quadrant of the patella (**Fig. 6**). The segmented fragment and the rest of the patella may articulate with each other via fibrotic or cartilaginous tissue. On MRI, the signal intensity between the segments will be low on all sequences due to the intervening fibrous tissue or high on fat suppressed intermediate weighted images due to the intervening cartilage or fluid [18, 19]. Caution is needed when there is signal alteration at either side of segmentation, indicative of bone marrow oedema, which is the result of friction and is usually painful. Plain radiographs reveal the sclerotic opposing borders

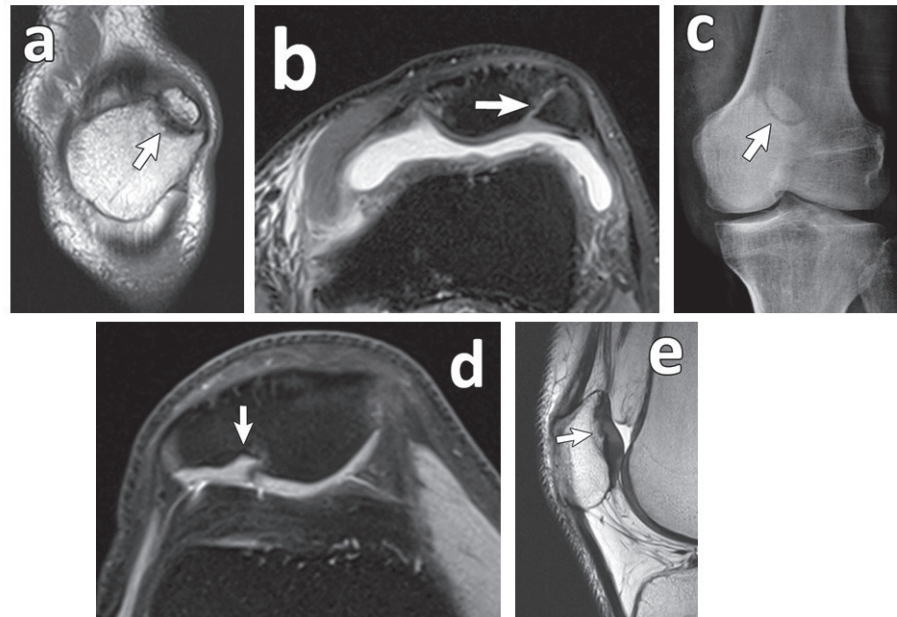


Fig. 6. **a:** coronal T1W, **b:** axial PDW with fat saturation, **c:** anteroposterior radiograph. A 66-year-old male patient with previous knee injury and torn medial collateral ligament. There is separation of the lateral upper part of the patella (arrows). High signal intensity is identified between the segmented fragments indicating a synchondrosis (arrow in **b**). Patellar cartilage is contiguous between the separated segments posteriorly, and the quadriceps tendon anteriorly the synchondrosis. Note the sclerotic opposing borders of the fragments on the radiograph (arrow in **c**). The findings are consistent with bipartite patella. **d:** axial PDW with fat saturation, **e:** sagittal T2W. A 51-year-old male patient with anterior cruciate ligament tear. There is signal alteration of the subchondral bone marrow at the posterior upper lateral part of the patella. The subarticular cortex has an anomalous border (arrows). The thickness of the overlying cartilage lies within normal limits. The findings are consistent with a dorsal defect of the patella.

of the segments consistent with unification failure and confirm the diagnosis [20].

The **dorsal defect of the patella** is considered an ossification variant of the posterior superolateral cortex [20]. The condition may deceive radiologists into considering an osteochondral lesion, but the overlying cartilage has normal signal intensity and its thickness remains within normal limits [19] (**Fig. 6**).

Intraarticular lesions

The **menisci** are wedged fibrocartilaginous structures, located between the femoral and tibial condyles. On MRI, meniscal tears are depicted as a high intrameniscal signal, especially on short TE sequences, traversing the substance of the meniscus extending to its surface [21]. Horizontal or oblique tears are frequently encountered in asymptomatic knees [22]. However, there are cases where this high signal line may not represent a tear but it is in fact a linear calcification within the meniscal substance. This finding is consistent with **chon-**

drocalcinosis of the meniscus [23]. Crystals of calcium pyrophosphate dihydrate, dicalcium phosphate dihydrate, calcium hydroxyapatite, or a combination of these are deposited in the menisci and/or the articular cartilage. According to Kaushic S. et al [24], in the presence of chondrocalcinosis, MRI will always misdiagnose a calcification as a meniscal tear. This can be avoided by correlating plain radiographs with the MRI examination (**Fig. 7**).

Discoïd meniscus is a congenital anomaly in which the meniscus covers the tibial plateau or a large part of it. The cross section of the meniscus is not triangular but it has a rounded trapezoidal shape, and the meniscus resembles a disc. A discoïd meniscus occurs almost exclusively at the lateral joint space. A medial location is very rare (less than 0.3%) [25]. Watanabe defines three anatomic types of discoïd menisci [26]: Type 1 (complete) is the most common and the meniscus covers the whole of lateral tibial plateau, and has a normal attachment to the capsule via the coronary ligament

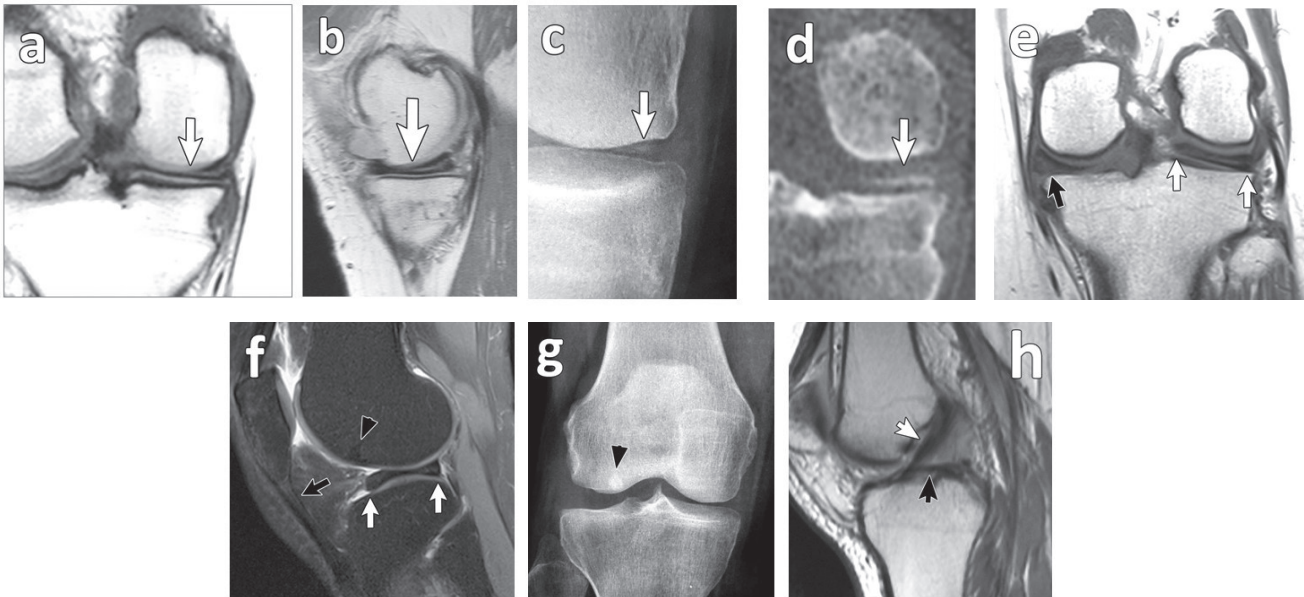


Fig. 7. **a:** coronal T1W, **b:** sagittal PDW, **c:** anteroposterior radiograph, **d:** coronal CT reformation. Male patient with knee injury. There is a high signal line in the posterior horn of the medial meniscus extending to the femoral surface of the meniscus (white arrows in **a** and **b**), consistent with a meniscal tear. However, review of the coronal radiograph and the coronal CT reformation shows that this line corresponds to a linear calcification of the meniscus (white arrows in **c** and **d**), consistent with chondrocalcinosis. **e:** coronal T1W, **f:** sagittal PDW with fat saturation, **g:** anteroposterior radiograph, **h:** sagittal PDW, are images of a 66-year-old female patient with knee pain and medial meniscus tear. The lateral meniscus has a rather trapezoid shape (white arrows in **e** and **f**), consistent with a discoid meniscus. There is a small amount of high signal within the meniscus, but it does not extend to its surface, which is consistent with mucoid degeneration. Note the diastasis of the lateral joint space at the corresponding radiograph. On the midline sagittal sequences, the discoid meniscus (black arrow in **h**) could be mistaken as a torn anterior cruciate ligament (arrow in **h**). Concomitant subarticular bone island (black arrowheads in **f** and **g**), degenerative medial meniscus tear (black arrows in **e**), tendinopathy of the patellar tendon (black arrow in **f**), and joint effusion are also present.

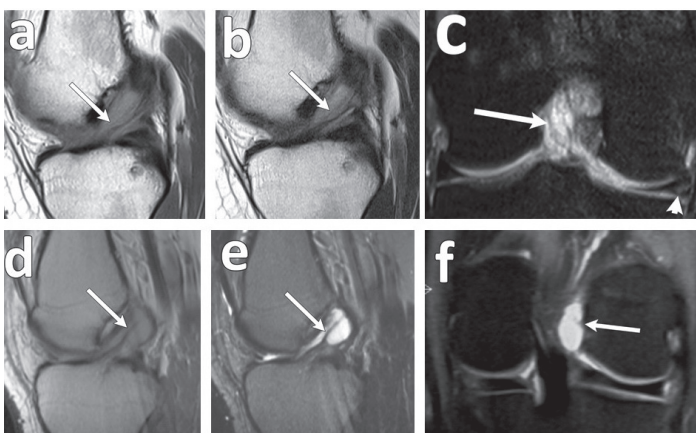


Fig. 8. **a:** sagittal PDW, **b:** sagittal T2W, **c:** coronal PDW with fat saturation. A 35-year-old female patient is followed up for chondromalacia. There is high signal in the ACL at the sagittal and coronal PDW images, which drops at the sagittal T2W image, below the fluid signal. Fibers are shown as low signal lines traversing the substance of the ACL (arrows in **a**, **b**, **c**), without disruption. The findings are consistent with mucoid degeneration of ACL. Concomitant peripheral tear of the medial meniscus (arrowhead in **c**). **d:** sagittal PDW, **e:** sagittal T2W, **f:** coronal PDW with fat saturation. A 21-year-old male patient with knee pain for a year. There is high signal in the ACL, which remains high on the T2W, consistent with fluid (compare with **b**). Fibers of the ligament are displaced but not disrupted. The findings are consistent with a ganglion cyst of the ACL.

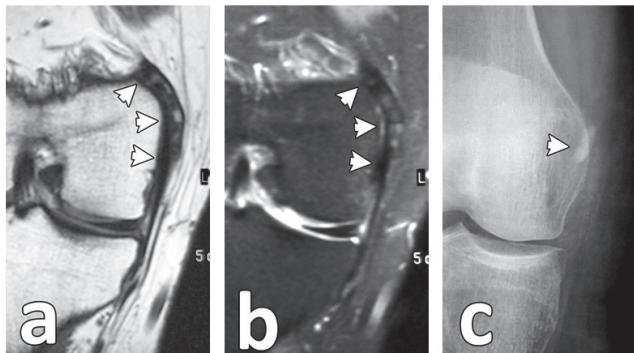


Fig. 9. a: coronal T1W, **b:** coronal PDW with fat saturation. Young male with anterior knee pain for a month. There is thickening of the femoral attachment of the medial collateral ligament (arrowheads). The signal intensity is inhomogeneous on T1W and PDW images. Findings are consistent with a Pellegrini-Stieda lesion. **c:** anteroposterior radiograph of another patient, in which the calcification at the femoral insertion of the MCL is clearly shown (arrowhead).

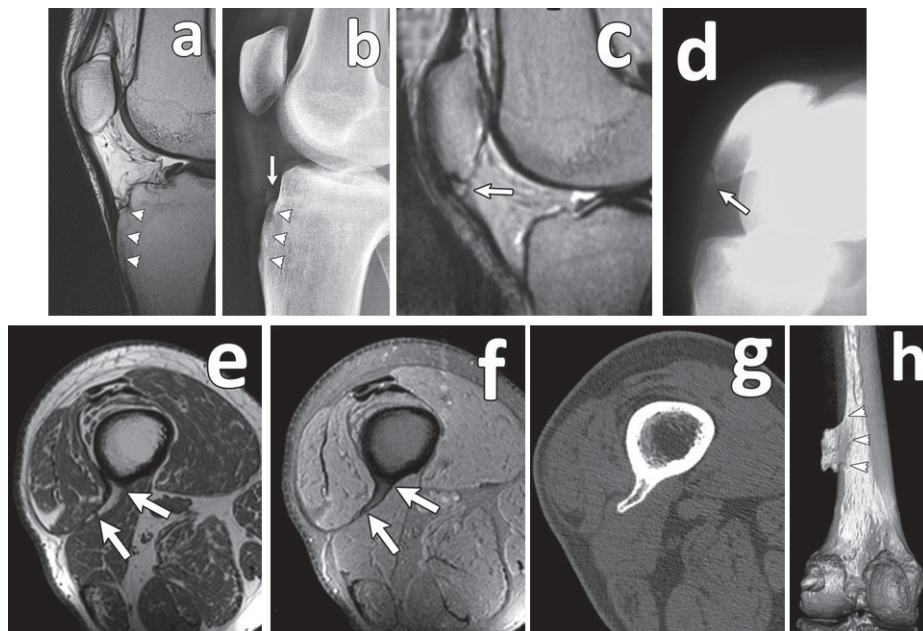


Fig. 10. a: sagittal PDW, **b:** lateral radiograph. A 25-year-old male patient with previous knee injury. The tibial tubercle is enlarged (arrowheads in **a** and **b**). There is a paratendinous focus of calcification, just above the insertion, clearly depicted on the plain radiograph (arrow in **b**). Findings are consistent with chronic Osgood-Schlatter disease. **c:** sagittal T2W, **d:** lateral radiograph. A 25-year-old female patient, with previous knee injury. At the patellar insertion of the patellar tendon, a focus of ossification is depicted (arrows). The adjacent Hoffa’s fat pad has normal signal intensity. Findings are consistent with chronic Sinding-Larsen-Johansson disease. **e:** axial T1W, **f:** axial T1W with fat saturation, **g:** axial CT, **h:** 3D CT reformation. A 65-year-old male patient, former soccer player. A lesion is revealed in continuity with the posterior cortex of the femoral bone (arrows in **e** and **f**). It has a low signal rim, in continuity with the osseous cortex. One may suspect an exostosis, but there is no continuation of the bone marrow with the center of the lesion, as this is clearly shown on the axial CT image. The cortex of the host femoral bone remains normal. The central portion of the lesion presents signal intensity equal to fatty marrow. On the 3D CT image the lesion is clearly shown to originate from the lateral ridge of the linea aspera (arrowheads in **h**), at the insertion of the tendon of vastus lateralis muscle. The findings are consistent with ossification of vastus lateralis muscle insertion.

(**Fig. 7**). Type 2 occupies less than 80% of the facet, and again it has a normal attachment to the capsule. Type 3 (Wrisberg type) has a more normal shape, with a thick posterior horn which connects only to the Wrisberg ligament, with no other posterior attachment. Discoid

menisci are prone to tearing secondary to increased thickness, poor tissue quality, and increased mobility in the case of discoid meniscus Type 3, due to lack of meniscocapsular attachment (snapping knee) [27]. An MRI classification was proposed by Ahn et al, based on

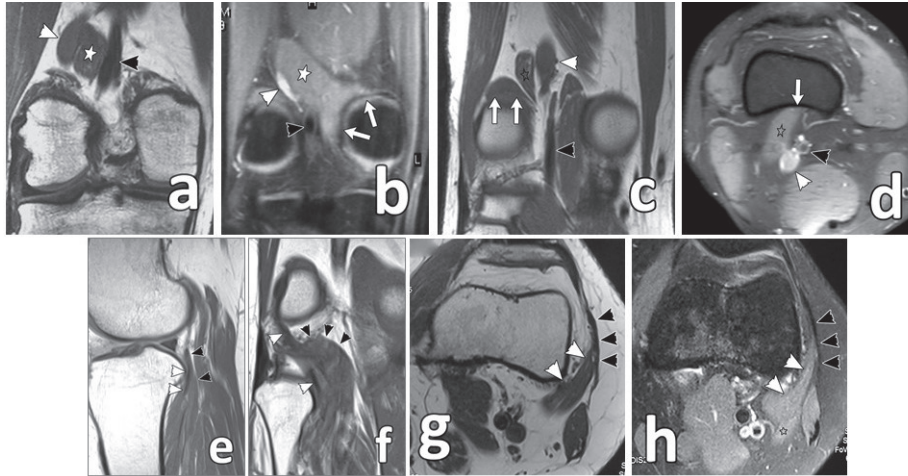


Fig. 11. a: coronal T1W, **b:** coronal PDW with fat saturation, posterior to **a**. A 18-year-old male patient, with knee injury. The structure (asterisk in **a**, **b**) located between the popliteal artery (black arrowhead in **a**, **b**) and vein (white arrowhead in **a**, **b**) has signal intensity equal to adjacent muscles, and blends posteriorly with the medial head of gastrocnemius muscle (arrows in **b**). Anteriorly it inserts into the lateral part of the posterior femoral surface. It represents an accessory split of the medial head of gastrocnemius muscle. These findings are consistent with Type III popliteal artery. **c:** coronal T1W, **d:** axial PDW with fat saturation. Male 38 years old, with knee pain. The structure (asterisk in **c** and **d**) located laterally of the popliteal artery (black arrowhead) and vein (white arrowhead) has signal intensity equal to adjacent muscles. Anteriorly it presents a broad insertion into the posterior surface of femur (arrow in **d**). It represents an accessory split of the lateral head of gastrocnemius muscle. The popliteal vessels are not compromised. **e:** sagittal PDW, **f:** coronal T1W. A 38-year-old female patient with knee injury. The tendon of the popliteal muscle (white arrowheads in **e** and **f**) is surrounded by muscle tissue up to the level of joint space. The abundant muscle tissue has a characteristic curved appearance on the coronal image (black arrowheads in **e** and **f**). The findings are consistent with a high belly of popliteal muscle. **g:** axial T1W, **h:** axial PDW with fat saturation lower than **g**. A 40-year-old female patient, with previous knee injury. There is a structure of muscle tissue signal intensity (white arrowheads in **g** and **h**) located between the lateral femoral condyle and the iliotibial band (black arrowheads in **g** and **h**). This muscle split is attached to the iliotibial band anteriorly, and posteriorly it blends with the belly of the plantaris muscle (asterisk in **h**). The findings are consistent with the presence of an accessory plantaris muscle.

the presence or direction of meniscal shift: no shift, anterocentral shift, posterocentral shift, and central shift [28]. This classification provides surgically relevant information. Attention should be paid not to diagnose meniscocapsular detachment in cases of a Type 3 discoid meniscus.

Unexpected MRI findings can be discovered at the **anterior cruciate ligament (ACL)**. On MRI the normal ACL is shown as a straight structure running parallel to the intercondylar notch and it manifests low signal intensity on all sequences [29]. In cases where intrasubstance high signal is depicted, with no definite history of trauma and the knee joint is clinically stable, two conditions should be included in the differential diagnosis. First, ACL may have undergone **mucoïd degeneration**. On MRI the ligament has high signal on T2W

images, as in a torn ACL, but the ligament's fibers are not disrupted and are shown as low signal linear structures traversing the substance of ACL [30] (**Fig. 8**). Second, the ACL may have developed a **ganglion cyst**. The signal intensity of the ganglion cyst is intermediate to low on T1W images and high (fluid) signal is revealed on T2W images, with distinct margins. The bands of the ACL are not disrupted but rather displaced by the ganglion. This latter finding distinguishes the ganglion cyst from mucoïd degeneration, although both lesions may coexist [30] (**Fig. 8**).

Extraarticular lesions

The MCL stabilises the knee against valgus stress. The stress may cause avulsion of the femoral attachment of the ligament and subsequent intratendinous calci-

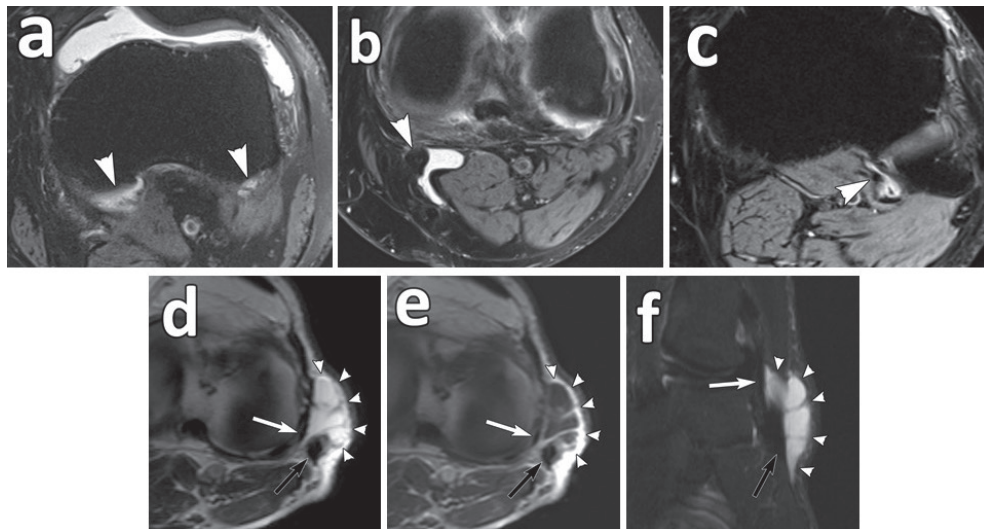


Fig. 12. axial PDW images with fat saturation at the level of femoral condyles (a), joint space (b), and head of fibula (c). A 50-year-old male patient, with recent knee injury. There is joint effusion. Distended bursae of the heads of gastrocnemius muscle (arrowheads in a), the semimembranosus tendon (arrowhead in b), and the popliteal muscle (arrowhead in c) are identified. d: axial T2W, e: axial T1W with contrast, f: coronal STIR. A 66-year-old male patient with previous knee injury. A cystic lesion (arrowheads in d, e, f) is identified in the subcutaneous tissue lateral to the joint space. It has a lobulated appearance and a few thin septae. It originates from the space between the lateral collateral ligament (white arrows in d, e, f) and the biceps femoris tendon (black arrows in d, e, f). The findings are consistent with a distended fibular collateral ligament-biceps femoris bursa.

fications may form. This is the classic description of a **Pellegrini-Stieda lesion**. Under exceptional valgus stress though (in cases of rupture of posterior cruciate ligament), stripping of the adjacent femoral periosteum may occur, and the subsequent calcification lies cephalad to MCL [31]. Pellegrini-Stieda is a chronic lesion and on MRI thickening of the femoral attachment of the ligament is shown [32]. The signal intensity is variable depending on the amount of calcium formed around the enthesis of the MCL [31] (**Fig. 9**). The calcifications are clearly depicted on the radiograph, confirming the Pellegrini-Stieda lesion.

Avulsion injuries may happen at **tendinous insertions** around the knee. At a chronic stage, MRI may reveal signal inhomogeneity at the insertions. Patellar tendon attachments are anatomic locations associated rather frequently with avulsions [33]. The avulsion injury of the ossification center of the tibial tuberosity during adolescence results in **Osgood-Schlatter disease**. The lesion is painful and calcification or even ossicle formation may be evident. When the pain subsides, these radiographic findings are the only sign of the disease [34]. On MRI the tendon insertion is thickened, the tibial tuberosity is enlarged and the ossicle presents

high signal intensity on T1W images, due to fatty marrow [34] (**Fig. 10**). With a similar mechanism, avulsion of the patellar insertion may occur after repetitive microtrauma, resulting in **Sinding-Larsen-Johansson disease**. Again, when the pain subsides, the only sign of the disease is the reactive intratendinous calcifications/ossifications. They are depicted clearly on plain radiographs [35] (**Fig. 10**). On MRI the tendon insertion is enlarged and the ossified areas demonstrate signal intensity similar to bone [36]. The insertion of the vastus lateralis muscle on the linea aspera may be a site of calcific tendinopathy. In the literature there are reports of lesions at the proximal insertion of the muscle [37, 38]. Similarly a **post-traumatic insertional ossification** of the peripheral attachment of the vastus lateralis muscle may occur (**Fig. 10**).

Accessory muscles around the knee joint are numerous [39]. On MRI the most characteristic feature is the similarity of the signal intensity with the adjacent muscles. The accessory splits of the medial and lateral gastrocnemius heads are among the frequently discovered accessory muscles on MRI of the knee. They are clinically important because they may compress the neighbouring popliteal vessels, and cause pain under

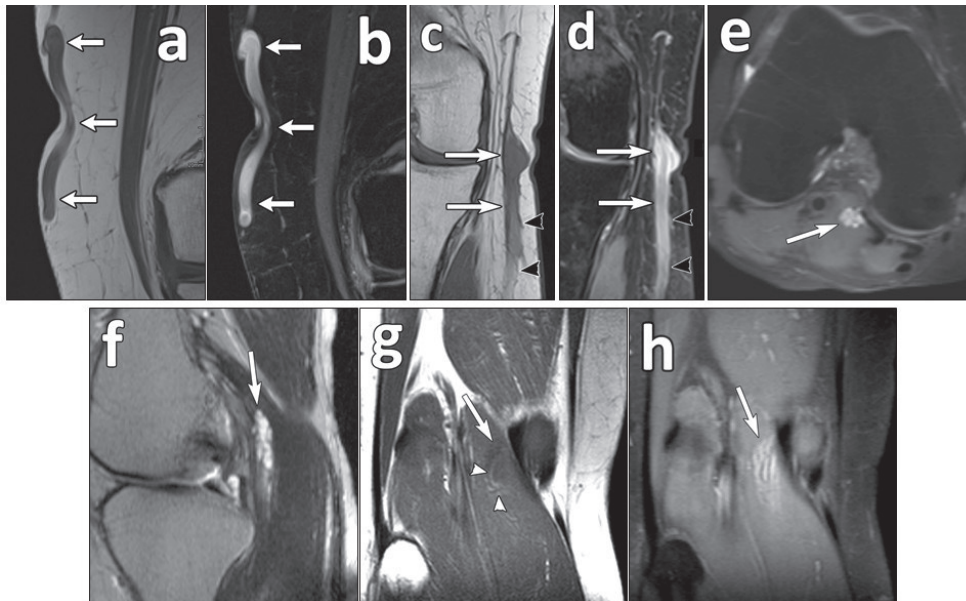


Fig. 13. a: coronal T1W, **b:** coronal PDW with fat saturation. A 59-year-old female patient, with knee injury. There is a long wavy structure (arrows in **a**, **b**), which presents low signal on the T1W and high on the PDW image. These are characteristic signs of a varicose vein. **c:** coronal T1W, **d:** coronal PDW with fat saturation. A 63-year-old female patient with anterior knee pain and degenerative arthritis. Incidentally discovered is a subcutaneous long straight structure (arrows in **c**, **d**). It has low signal intensity on the T1W and high on the PDW image. The lumen of the vein, caudally, shows high signal intensity on the T1W image and high signal, respectively, on the PDW image (arrowheads in **c** and **d**). These findings are consistent with a partially thrombosed vein. **e:** axial PDW with fat saturation, **f:** sagittal T2W, **g:** coronal T1W, **h:** coronal PDW with fat saturation. A 46-year-old female patient, follow-up for chondromalacia. There is a lesion in the belly of lateral head of the gastrocnemius muscle (arrows in **e**, **f**, **g**, **h**), with lobulated distinct margin. It has high signal intensity on T2 and PDW fat saturated images. There are thin low signal septae traversing the lesion. Inside the lesion, there are dispersed areas of moderate high signal (arrowheads in **g**), consistent with adipose tissue. Findings are in accordance with an intramuscular haemangioma.

active flexion due to ischaemia [39, 40] (**Fig. 11**). The popliteal muscle may have a highly located belly. This belly extends upwards, surrounding the tendon at the level of the joint space or even above it. This variation was present in 3 out of 23 patients in the series of Burman [41], and it is not infrequent in our experience as well. On MRI, the popliteal tendon is surrounded by muscle tissue up to or higher than the joint space (**Fig. 11**). In cases of surgical correction of varus instability, the popliteal tendon is used to reinforce the fibular collateral ligament. So this muscle variation may be of significance in cases of surgical management of the lateral compartment of the knee [41]. The accessory plantaris muscle is a recently described muscle that anteriorly inserts onto the lateral tibial band and posteriorly blends with the lateral gastrocnemius muscle [42, 43] (**Fig. 11**). It is situated between the iliotibial band and the lateral femoral condyle, thus restricting the ability of the in-

terspaced adipose tissue to absorb the pressure of the iliotibial band onto the lateral femoral condyle. Therefore, it may play a role in causing iliotibial band friction syndrome.

There are a number of **bursae** communicating with the joint cavity, and are filled with joint fluid in cases of joint effusion. Common locations include the suprapatellar bursa, around the semimembranosus tendon, at the insertions of the heads of gastrocnemius muscle, and the popliteal muscle tendon [44] (**Fig. 12**). However, there are bursae that do not communicate with the joint cavity, and are usually collapsed. They may enlarge due to repetitive friction and cause symptoms, but they are accidentally discovered as well. An example is the distended fibular collateral ligament-biceps femoris bursa (**Fig. 12**). As expected, these bursae will present with low to intermediate signal intensity on T1W images and high signal intensity on T2W images. Only the pe-

riphery of the bursa will enhance following intravenous contrast injection [44].

Finally, we would like to discuss the incidental findings associated with **vessels** around the knee. **Varicose veins** may be present. They may be occluded, causing discomfort and pain, but in the vast majority the only complaint is their cosmetic appearance [45] (**Fig. 13**). Subcutaneous **venous aneurysms** are uncommon, usually acquired, lesions and they most frequently present clinically as painless protruding lumps. When imaging is needed, ultrasound will clearly show not only the size of the aneurysm, but also the presence of a thrombus [46]. It is important to note that superficial vein thrombosis and thrombosed venous aneurysms can be associated with deep vein thrombosis and pulmonary embolism [46, 47]. So thrombosed varicose veins and aneurysms should be specifically noted in the report.

Haemangiomas represent accumulation of abnormally multiplied vessels. Histologically they consist of thick-walled vessels with phleboliths, smooth muscle, and reactive overgrowth of fat. Intramuscular haemangiomas have an incidence of approximately 7% of soft tissue tumours. If they are small they do not cause symptoms. They tend to enlarge overtime and if they become sufficiently large, they may cause symptoms and restriction of muscle function [48]. On MRI, the lesion appears lobulated, with high signal intensity on T2W images. However, parts of the lesion present high signal compared to that of skeletal muscle on T1W images due to fat content (**Fig. 13**). Low signal foci on all sequences are attributed to phleboliths. All lesions enhance after intravenous injection of gadolinium [48].

Conclusion

In this pictorial essay we present our experience of unexpected findings on knee MRI examinations, not related to patient’s symptoms. Radiologists should carefully inspect all the anatomical structures so that incidental findings are recognised. Although in the vast majority of cases, these incidental findings are not clinically significant, notable exceptions exist. Unexpected bone tumours need cautious interpretation as they may have malignant potential, or, if sufficiently enlarged, may cause weakening of bone and subsequent fracture. Bone marrow and menisci may reveal findings of systemic conditions. Discoid meniscus is important information for the arthroscopist. Congenital anomalies of the patella should be correctly differentiated from fracture and chondromalacia. The high signal intensity within the ACL, in the absence of previous injury, should be inspected for signs of ganglion cyst or mucoid degeneration. Attention should be given to tendons and ligaments insertions, as they may reveal findings of previous avulsions, and increased risk of future tear. Aberrant muscles should be reported because of their potential clinical and surgical implications. Bursae should be noted, especially if they do not communicate with the joint cavity. Careful inspection of the subcutaneous tissue and muscles is needed for revealing probable vessels’ anomalies. Finally, we emphasise the importance of interpreting knee MRI examinations in tandem with plain radiographs (or/and CT) in order to identify typical manifestations of lesions (sclerotic margins, calcifications-ossifications, phleboliths), either in the bones or in the soft tissues. **R**

REFERENCES

1. Resnick D, Niwayama G. Enostosis (Bone Island). In: Resnick D & Niwayama G (Eds). *Diagnosis of bone and joint disorders*. WB Saunders Company, Philadelphia 1988, pp 4074-4088.
2. Mugerá C, Suh JK, Huisman AGMT, et al. Sclerotic lesions of the spine: MRI assessment. *J Magn Reson Imaging* 2013; 38: 1310-1324.
3. Resnick D, Niwayama G. Enostosis (Bone Island). In: Resnick D & Niwayama G (Eds). *Diagnosis of bone and joint disorders*. WB Saunders Company, Philadelphia 1988, pp 3679-3688.
4. Stomp W, Reijnierse M, Kloppenburg M, et al. Prevalence of cartilaginous tumours as an incidental finding on MRI of the knee. *Eur Radiol* 2015; 25: 3480-3487.
5. Resnick D, Niwayama G. Enostosis (Bone Island). In: Resnick D & Niwayama G (Eds). *Diagnosis of bone and joint disorders*. WB Saunders Company, Philadelphia 1988, pp 3701-3720.
6. Resnick D, Niwayama G. Enostosis (Bone Island). In: Resnick D & Niwayama G (Eds). *Diagnosis of bone and joint disorders*. WB Saunders Company, Philadelphia 1988, pp 3739-3746.
7. Herget GW, Mauer D, Krauß T, et al. Non-ossifying fibroma: natural history with an emphasis on a stage-related growth, fracture risk and the need for follow. *BMC Musculoskelet Disord* 2016; 17: 147.
8. Jee WH, Choe BY, Kang HS, et al. Nonossifying fibroma: Characteristics at MR imaging with pathologic correlation. *Radiology* 1998; 209: 197-202.
9. Muzykewicz DA, Goldin A, Lopreiato N, et al. Non-ossifying fibromas of the distal tibia: possible etiologic relationship to the interosseous membrane. *J Child Orthop* 2016; 10: 353-358.
10. Ritschl P, Karnel F, Hajek P. Fibrous metaphyseal defects—determination of their origin and natural history using a radiomorphological study. *Skeletal Radiol* 1988; 17(1): 8-15.
11. La Rocca Vieira R, Bencardino TJ, Rosenberg ZS, et al. MRI features of cortical desmoid in acute knee trauma. *AJR Am J Roentgenol* 2011; 196: 424-428.
12. Tscholl MP, Biedert MR, Gal I. Cortical desmoids in adolescent top-level athletes. *Acta Radiol Open* 2015; 4(5): 1-5.
13. Resnick D, Niwayama G. Enostosis (Bone Island). In: Resnick D & Niwayama G (Eds). *Diagnosis of bone and joint disorders*. WB Saunders Company, Philadelphia 1988, pp 3782-3786.
14. Campbell RSD, Grainger AJ, Mangham DC, et al. Intraosseous lipoma: report of 35 new cases and a review of the literature. *Skeletal Radiol* 2003; 32: 209-222.
15. Levin FM, Alexander D, Vellet DA, et al. Intraosseous lipoma of the distal femur: MRI appearance. *Skeletal Radiol* 1996; 25: 82-84.
16. Malkiewicz A, Dziedzic M. Bone marrow reconversion – imaging of physiological changes in bone marrow. *Pol J Radiol* 2012; 77(4): 45-50.
17. Ogden JA. Radiology of postnatal skeletal development. X. Patella and tibial tuberosity. *Skeletal Radiol* 1984; 11: 246-257.
18. Kavanagh EC, Zoga A, Omar I, et al. MRI findings in bipartite patella. *Skeletal Radiol* 2007; 36: 209-214.
19. Vanhoenacker F, De Vos N, Van Dyck P. Common mistakes and pitfalls in Magnetic Resonance Imaging of the knee. *J Belg Soc Radiol* 2016; 100(1): 99: 1-17.
20. Van Holsbeeck M, Vandamme B, Marchal G, et al. Dorsal defect of the patella: concept of its origin and relationship with bipartite and multipartite patella. *Skeletal Radiol* 1987; 16: 304-311.
21. De Smet AA. How I diagnose meniscal tears on knee MRI. *AJR Am J Roentgenol* 2012; 199: 481-499.
22. Zanetti M, Pfirrmann CWA, Schmid MR, et al. Patients with suspected meniscal tears: prevalence of abnormalities seen on MRI of 100 symptomatic and 100 contralateral asymptomatic knees. *AJR Am J Roentgenol* 2003; 181: 635-641.
23. Burke BJ, Escobedo EM, Wilson AJ, et al. Chondrocalcinosis mimicking a meniscal tear on MR Imaging. *AJR Am J Roentgenol* 1998; 170: 69-70.
24. Kaushik S, Erickson JK, Palmer WE, et al. Effect of chondrocalcinosis on the MR Imaging of knee menisci. *AJR Am J Roentgenol* 2001; 177: 905-909.
25. Kim JG, Han SW, Lee DH. Diagnosis and treatment of discoid meniscus. *Knee Surg Relat Res* 2016; 28(4): 255-262.
26. Watanabe M, Takeda S, Ikeuchi H. Atlas of arthroscopy. Igaku-Shoin, Tokyo 1979, pp 75-130.
27. Kocher MS., Logan CA, Kramer DE. Discoid lateral

- meniscus in children: Diagnosis, management, and outcomes. *J Am Acad Orthop Surg* 2017; 25(11): 736-743.
28. Ahn JH, Lee YS, Ha HC, et al. A novel magnetic resonance imaging classification of discoid lateral meniscus based on peripheral attachment. *Am J Sports Med* 2009; 37: 1564-1569.
 29. Domnick C, Raschke MJ, Herbort M. Biomechanics of the anterior cruciate ligament: Physiology, rupture and reconstruction techniques. *World J Orthop* 2016; 7(2): 82-93.
 30. Vaishya R, Esin Issa A, Agarwal A, et al. Anterior cruciate ligament ganglion cyst and mucoid degeneration: A review. *Cureus* 2017; 9(9): e1682. doi:10.7759/cureus.1682.
 31. McAnally JL, Southam SL, Mlady GW. New thoughts on the origin of Pellegrini-Stieda: the association of PCL injury and medial femoral epicondylar periosteal stripping. *Skeletal Radiol* 2009; 38: 193-198.
 32. Madani H, Tincey S, Tavare AN, et al. Chronic MCL syndrome: anatomy, pathology, clinical presentation and treatment. Available via <http://dx.doi.org/10.1594/ecr2015/C-2071>. Published on 2015.
 33. Gottsegen JC, Eyer BA, White EA, et al. Avulsion fractures of the knee: Imaging findings and clinical significance. *Radiographics* 2008; 28: 1755-1770.
 34. Hirano A, Fukubayashi T, Ishii T, et al. Magnetic resonance imaging of Osgood-Schlatter disease: the course of the disease. *Skeletal Radiol* 2002; 31: 334-342.
 35. Dupuis SC, Westra SJ, Makris J, et al. Injuries and conditions of the extensor mechanism of the pediatric knee. *Radiographics* 2009; 29: 877-886.
 36. Levin ES, Motamedi K, Plotkin B, et al. All about the patella: Not just a cap for the knee. Available via <http://dx.doi.org/10.1594/ecr2017/C-0585>. Published on 2017.
 37. Ramon FA, Degryse HR, De Schepper AM, et al. Calcific tendinitis of the vastus lateralis muscle. A report of three cases. *Skeletal Radiol* 1991; 20: 21-23.
 38. Low SBL, Toms AP. Calcification of the linea aspera: A systematic narrative review. *Eur J Radiol Open* 2019; (6): 101-105.
 39. Sookur PA, Naraghi AM, Bleakney RR, et al. Accessory muscles: Anatomy, symptoms, and radiologic evaluation. *Radiographics* 2008; 28: 481-499.
 40. Pikoulas K, Mantzikopoulos G, Giannikouris G, et al. Type III popliteal artery due to split of medial gastrocnemius muscle. Available via <https://www.eurorad.org/case/11790>. Published on June 27, 2014.
 41. Michael Burman. The High-bellied popliteus muscle. *JBJS Am* 1968; 50 (4): 761.
 42. Pikoulas K, Staikidou I, Giannikouris G, et al. Accessory plantaris muscle. Pictorial review and clinical implications. Available via <http://dx.doi.org/10.1594/essr2018/P-0002>. Published on 2018.
 43. Herzog RJ. Accessory plantaris muscle: Anatomy and prevalence. *Hosp Spec Surg J* 2011; 7: 52-56.
 44. Perdikakis E, Skiadas V. MRI characteristics of cysts and “cyst-like” lesions in and around the knee: what the radiologist needs to know. *Insights Imaging* 2013; 4: 257-272.
 45. Campbell B. Varicose veins and their management. *BMJ* 2006; 333: 287-292.
 46. Mckesey J, Cohen PR. Spontaneous venous aneurysm: Report of a non-traumatic superficial venous aneurysm on the distal arm. *Cureus* 2018; 10(5): e2641. doi: 10.7759/cureus.2641
 47. Nasr H, Scriven JM. Superficial thrombophlebitis (superficial venous thrombosis). *BMJ* 2015; 350: h2039.
 48. Griffin N, Khan N, Thomas JM, et al. The radiological manifestations of intramuscular haemangiomas in adults: magnetic resonance imaging, computed tomography and ultrasound appearances. *Skeletal Radiol* 2007; 36: 1051-1059.



READY-MADE
CITATION

Pikoulas K, Giannikouris G, Staikidou I, Mantzikopoulos G. “Incidentalomas” on MR imaging examinations of the adult knee. A pictorial essay. *Hell J Radiol* 2021; 6(2): 44-57.